

ISSN: 0976-3031

*International Journal of Recent Scientific
Research*

Impact factor: 5.114

**NONUNIFORMLY DISTRIBUTED FLOW PATTERNS AFTER
MELODY® IMPLANTATION: IMPLICATIONS FOR FOCAL
ELEVATED PULMONARY WALL SHEAR RATES AND
RIGHT VENTRICULAR FUNCTION**



**Soha Romeih., Rob J. Van Der Geest., Arno AW Roest., Anje M
Spijkerboer., Mark G Hazekamp., Barbara JM Mulder., Nico A
Blom and Maarten Groenink**

Volume: 6

Issue: 10

**THE PUBLICATION OF
INTERNATIONAL JOURNAL OF RECENT SCIENTIFIC RESEARCH**

<http://www.recentscientific.com>

E-mail: recentscientific@gmail.com



ISSN: 0976-3031

Available Online at <http://www.recentscientific.com>

International Journal of Recent Scientific Research
Vol. 6, Issue, 10, pp. 6774-6780, October, 2015

*International Journal
of Recent Scientific
Research*

RESEARCH ARTICLE

NONUNIFORMLY DISTRIBUTED FLOW PATTERNS AFTER MELODY® IMPLANTATION: IMPLICATIONS FOR FOCAL ELEVATED PULMONARY WALL SHEAR RATES AND RIGHT VENTRICULAR FUNCTION

Soha Romeih*^{1,8}, Rob J. Van Der Geest², Arno AW Roest³, Anje M Spijkerboer¹, Mark G Hazekamp⁴, Barbara JM Mulder^{5,7}, Nico A Blom^{3,6} and Maarten Groenink^{1,5,7}

¹Department of Radiology, Academic Medical Center, Amsterdam, the Netherlands

²Department of Radiology, Leiden University Medical Center, Leiden, the Netherlands

³Department of Pediatrics, Leiden University Medical Center, Leiden, the Netherlands

⁴Department of Cardiothoracic Surgery, Academic Medical Center, Amsterdam, the Netherlands

⁵Department of Cardiology, Academic Medical Center, Amsterdam, the Netherlands

⁶Department of Pediatrics, Academic Medical Center, Amsterdam, the Netherlands

⁷Interuniversity Cardiology Institute of the Netherlands, Utrecht, the Netherlands

⁸Department of Cardiology, Tanta University Hospital, Tanta, Egypt

ARTICLE INFO

Article History:

Received 06th July, 2015

Received in revised form

14th August, 2015

Accepted 23rd September, 2015

Published online 28st

October, 2015

Key words:

4D pulmonary flow, Melody® valve, Contegra® conduit.

ABSTRACT

Background: Turbulent flow patterns distal to Melody® valves are frequently observed by standard performed MRI. These turbulent flow patterns may have an impact on RV afterload conditions and RV function. The aim of this study was to compare pulmonary flow patterns between patients who underwent Melody® and Contegra® implantation and the impact of these flow patterns on pulmonary wall shear rates and right ventricular morphology and function.

Patients and Methods: Fifteen patients after Melody® valve implantation (17.2 ± 2.0 years), 15 patients after Contegra® implantation (15.8 ± 1.7 years), and 15 healthy volunteers, as a control group, (16.5 ± 1.5 years) were included. All subjects underwent a comprehensive cardiac MRI protocol, assessing RV morphology, function, pulmonary flow and vortices. From 3D flow analysis pulmonary flow eccentricity and pulmonary wall shear rate (WSR) were calculated.

Results: Patients in the Melody® group showed reduced RVEF as compared to controls, eccentric pulmonary flow (deviation angle from the midline $31 \pm 10^\circ$) with vortex formation (vortex size 73 ± 18 %), and a significant asymmetric elevated WSR at focal regions of the conduit. In contrast, those after surgical Contegra® implantation showed a laminar pulmonary flow with no visible vortex and had symmetric, although elevated WSR in all conduit regions and an RV function comparable to controls.

Conclusion: Unfavorable pulmonary flow patterns with vortex formation distal from the Melody® valve lead to abnormal hemodynamic conditions that may influence RV function and might be a predisposing factor for pulmonary aneurysm formation.

Copyright © Soha Romeih *et al.* 2015, This is an open-access article distributed under the terms of the Creative Commons Attribution License, which permits unrestricted use, distribution and reproduction in any medium, provided the original work is properly cited.

INTRODUCTION

Pulmonary valve stenosis and/or incompetence are common problems in patients after correction of congenital heart diseases.^{1,2} Prolonged pressure or volume overload may lead to irreversible right ventricular (RV) dysfunction.³ Therefore, right ventricular outflow tract (RVOT) repair by surgical implantation of a bovine jugular venous valve (Contegra® conduit) or a pulmonary homograft is commonly performed.⁴ Recently, percutaneous implantation of the same bovine jugular venous valve, sutured to a balloon-expandable platinum iridium

stent (Melody® valve) has become a less invasive solution for patients with dysfunction of a homograft in the RVOT position. Herewith, the number of open-heart surgeries these patients have to undergo in their life may be reduced.⁵⁻⁷ Although mid-term follow-up of patients who underwent percutaneous bovine valve implantation seems to be satisfactory,^{6,8} turbulent flow patterns distal to the valve are often seen. (Figure 1) Recently, time resolved three dimensional magnetic resonance velocity mapping, also known as 4D flow, has gained considerable interest.^{9,10} By application of this technique it is feasible to assess blood flow velocities in all directions while simultaneously providing morphological information, which

*Corresponding author: Soha Romeih

Department of Radiology, Academic Medical Center, Amsterdam, the Netherlands

allows detailed insights into the local blood flow dynamics. In addition, 4D flow allows calculation of the wall shear rate (WSR) i.e., the force per unit area induced by the relative movement of blood at the endothelium, in the vessel upstream from the valve, which is considered an important determinant for vascular remodeling.¹¹⁻¹³ We investigated RV morphology, RV function and 4D flow dynamics in patients with a percutaneously implanted bovine jugular venous valve (Melody® valve) and compared these parameters with patients who underwent surgical implantation of the bovine jugular venous valve (Contegra® conduit). We hypothesized that disturbed flow patterns would be more frequently present and that WSRs would be higher in patients with a percutaneously implanted bovine jugular venous valve (Melody® group) than in patients with a surgically implanted bovine jugular venous valve (Contegra® group). Furthermore, we hypothesized that these unfavorable afterload conditions might influence RV morphology and function.

PATIENTS AND METHODS

Informed consent was obtained from all participants and/or parents prior to enrolment. Patients who underwent Melody® valve implantation at our institutions, older than 8 years, and without contra-indications for MRI examination, were included in the study. Patients were retrospectively recruited from the pediatric cardiology database of the “Center for Congenital Heart Disease Amsterdam Leiden” (www.CAHAL.nl). The database showed 15 eligible patients (8 male, 17.2 ± 2.0 years). Fifteen age and sex matched patients after Contegra® conduit implantation (10 male, 15.8 ± 1.7 years) and 15 age and sex matched healthy volunteers (6 male, 16.5 ± 1.5 years), as a control group, were included. All subjects underwent a standard echocardiographic examination using a Vivid 7.0.0 machine (GE Vingmed Ultrasound AS, Horten, Norway) to assess the maximum flow velocity (Vmax) of the pulmonary flow and a comprehensive cardiac MRI protocol including 4D flow assessment across the pulmonary/conduit valve.

Cardiac MRI

Cardiac MRI was performed on a Philips Panorama 1.0 T open MRI scanner (Panorama, Philips Medical Systems, Best, the Netherlands). Two and 4-chamber views, RVOT views in two orthogonal planes, and short-axis views consisting of 12 to 14 contiguous slices, covering both ventricles from the base of the heart till the apex were acquired using a retrospective ECG-gated steady-state free precession sequence during breath holding at end-expiration. For choosing a correct velocity-encoded MRI in the 4D MRI flow sequence, the flow across the pulmonary/conduit valve was first assessed using a free-breathing retrospective 2D ECG-gated through plane velocity encoded MRI. Scan parameters were: TR/TE 9/5 msec, FOV 370 – 400 mm, flip angle (FA) 15 - 20°, slice thickness 6-8 mm, matrix 128 x 256, temporal resolution approximately 20 msec. Standard velocity encoding of 1.5 m/sec was initially chosen. When a higher velocity encoding was required based on the 2D velocity encoded sequence, this higher velocity encoding was used for the 4D flow acquisition.

For 4D flow mapping, a 60-mm slab was placed at the RVOT, from the pulmonary valve to the pulmonary bifurcation, verified to encompass this region throughout the cardiac cycle (this was visually verified in the two orthogonal views of the RVOT). Velocity was encoded in three orthogonal directions and the images were acquired during free breathing by an imaging sequence with retrospective gating (10% acceptance window, 30 reconstructed cardiac phases). Imaging parameters were as follows: TR/TE 9.3/5.2 msec, FOV 370 – 400 mm, FA 10°, acquisition voxel size: $2 \times 2 \times 4.0$ mm, reconstructed into a voxel size of $1.2 \times 1.2 \times 4.0$ mm, two signal averages, and a 237 Hz sampling bandwidth. The 60-mm slab was reconstructed into 15 sections of 4 mm thickness.

Image post-processing

Right ventricular systolic function and mass were analyzed using the MASS® research software package (Version V2012-EXP, Leiden University Medical Center, the Netherlands). The RV systolic function was assessed by drawing endocardial contours at end-systole and end-diastole in all sections of the cine short axis data to obtain end-systolic volume (ESV), end-diastolic volume (EDV), stroke volume (SV) and ejection fraction (EF). An RVEF < 47% was defined as abnormal.^{14;15} RV mass was assessed by drawing RV epicardial borders for each slice level where the area of the interventricular septum was allocated to the LV. Masses were summed from apex to base with subsequent indexation for body surface area. A RV mass > 22 g/m² was defined as a hypertrophied RV.^{14;15} Diameters of the pulmonary artery/conduit were assessed as the mean of two measurements of the RVOT in two orthogonal cine imaging view at the pulmonary valve level, in the Melody group at the mid of the stent: D_{proximal} , just before the bifurcation: D_{distal} , and at half the distance between the pulmonary artery and the bifurcations: D_{mid} . In the Contegra® group, the symmetry of the conduit valve opening was visually assessed, while this was not possible in the Melody® group due to the stent artifacts. Pulmonary artery/conduit distension (P_{mid}) was measured at the location of D_{mid} as the difference between pulmonary artery/conduit area in the peak systolic and in the early diastolic phase. Flow patterns were qualitatively and quantitatively assessed using color-coded streamlines visualization in both orthogonal RVOT views in each individual time frame. All traces were color-coded according to the local blood flow velocity.^{16;17}

Analysis focused on the presence of vortices and eccentricity of the pulmonary flow. A vortex was defined as particles revolving around a point within the vessel with a rotation direction deviating by more than 90° from the physiological flow direction. The relative period of the vortex existence (number of cardiac phases with vortex divided by the total number of imaged cardiac phases) was determined visually. The vortex size was measured as a percentage of the vessel diameter in the phase showing the maximal diameter of the vortex. Eccentric pulmonary flow jets were defined as predominantly peripheral high-velocity vectors, away from the pulmonary artery midline; the flow deviation angle from the midline was measured. Pulmonary flow quantification was directly derived from the measured 4D flow data and measured

at the location of D_{mid} (half the distance between the pulmonary valve and the bifurcation) in the control and the Contegra® groups. In the Melody® group pulmonary flow was quantified just distally to the stent to avoid stent artifacts, in all patients approximately at the same level as in the other groups. A reformatting plane was generated perpendicular to the pulmonary artery/conduit on both orthogonal RVOT cine views. The 4D velocity encoded images were reformatted to yield 30 through-plane velocity-encoded images with which the flow analysis was performed. For each phase the luminal border was traced and flow velocity curves were derived by multiplying the lumen area in each time frame by the average flow velocity to yield the following parameters: pulmonary forward flow volume, pulmonary backward flow volume, and pulmonary effective flow volume (forward minus backward flow volume), and pulmonary V_{max} .¹⁸ WSRs were measured at the same site of the reformatting plane in the phase of maximum velocity as described by the *Stalder et al.*¹⁹ WSRs were calculated at four local anatomical positions starting from the pulmonary artery/ conduit wall facing the aorta (aorta wall), anterior wall, lateral wall, and posterior wall. (Figure 2)

Statistical Analysis

A one-way analysis of variance (ANOVA) was used to analyze differences in quantitative parameters between groups. Post hoc least significant difference (LSD) testing was performed for parameters that proved statistically significant on ANOVA. The Pearson correlation coefficient was calculated to evaluate the potential correlation between RV systolic function, RV mass, time after Contegra® conduit and Melody® valve implantation, pulmonary artery/conduit diameters, pulmonary artery/ conduit distension, pulmonary flow deviation angle, vortex existence, vortex size, pulmonary V_{max} , and WSRs. P-values less than 0.05 were considered significant. SPSS® version 20 was used for statistical analysis.

RESULTS

Patient characteristics

Baseline data are summarized in Table 1. All patients were in New York Heart Association (NYHA) class I or II and received no medication. Melody® valves were implanted in homografts (time from implantation 13.5 ± 4 years); one patient (7%) had a second Melody® valve implantation. In the Contegra® group, five patients (33%) had a replacement of the Contegra® conduit after previous Contegra® placement.

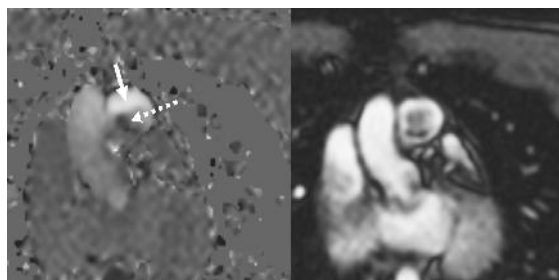


Figure 1 2D through plane flow just above the Melody® valve demonstrating turbulent flow with both forward (solid arrow) and backward (dashed arrow) directed flow during systole. Phase contrast image (left) and modulus image (right).

Table 1 Baseline data over the Patients characteristics

Parameter	Contegra® group (15 patients)	Melody® group (15 patients)
Age (years ± SD)	15.8 ± 1.7	17.2 ± 2.0
Diagnosis		
TOF-PA/VSD	7 (47%)	8 (53%)
PA/IVS	1	2
Rastelli operation	3	2
Ross operation	4	3
Number of thoracotomies		
One thoracoatomy	0	3
Two thoracotomies	10	12
Three thoracotomies	5	0
NYHA classification		
I	10 (67%)	9 (60%)
II	5 (33%)	6 (40%)

TOF: Tetralogy of Fallot, PA/VSD: pulmonary atresia and ventricular septum defect, PA pulmonary atresia and intact ventricular septum

Time after Contegra® conduit implantation was 7.4 ± 4.3 years, and after Melody® valve implantation was 2.9 ± 1.3 years, ($p < 0.001$). All patients successfully underwent cardiac MRI examination.

Comparison between the three groups

Results are summarized in Table 2. Patients in the Contegra® and the Melody® groups had a normal RV systolic function. However, RV-EF in the Melody® group was significantly lower than in the control group. Both the Contegra® and the Melody® groups showed RV hypertrophy and the RV mass was comparable in both groups. No correlation between RV-EF and time after Contegra® conduit implantation ($R = -0.17$, $p = 0.5$) or Melody® valve implantation ($R = 0.01$, $p = 0.9$) was observed.

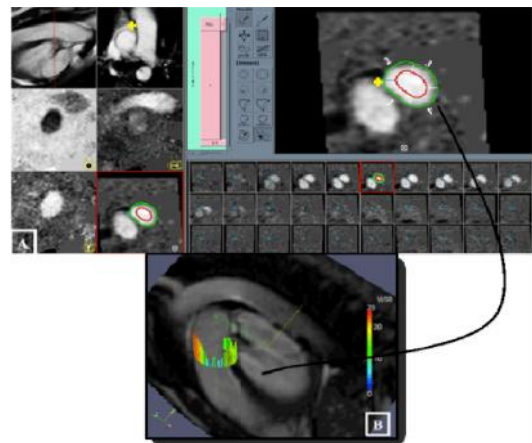


Figure 2 (A) Quantification of wall shear rates (WSRs) in the phase of maximum velocity (phase 6), the luminal boundary of the pulmonary artery (green contour) was drawn and a concentric contour was generated automatically at a fixed distance of 5 mm inside the lumen (red contour). Radial velocity profiles within the region defined by the two contours were analysed to obtain local WSR values. WSRs were calculated at four local anatomical positions starting from the pulmonary wall facing the aorta (at the yellow cross) aorta wall (1), anterior wall (2), lateral wall (3), and posterior wall (4). (B) WSRs measurements.

The conduit diameters were smaller in the Contegra® group as compared to the Melody® and the control groups. Conduit distension was lower in the Contegra® group. (Table 2) Thirteen patients in the Contegra® group (87%) showed

symmetrical opening of the conduit valve, while 2 patients (13%) showed an asymmetrical valve opening. None of the subjects had clinically relevant pulmonary valve incompetence. Contegra® group patients had a significantly lower pulmonary Vmax, measured by 4D flow, as compared to those with Melody® valve (2.6 ± 0.6 m/sec vs. 3.3 ± 0.6 m/sec respectively, p = 0.009).

In the Contegra® group, WSRs were symmetrical, but elevated, compared to the control and the Melody® groups (Table 2, Figure 5). In the Melody® group, the anterior wall WSR was elevated whereas the other wall regions (lateral, posterior, and aorta wall) showed no differences in comparison with the control group. (Table 2) There was no correlation between WSRs and pulmonary Vmax in the three groups.

Table 2 Comparison of MRI data between the three groups

Parameter	Control group (15 subjects)	Contegra® group (15 patients)	Melody® group (15 patients)	P value (Between Contegra® and control groups)	P value (Between Melody® and control groups)	P value (Between Melody® and Contegra® groups)
RV-EF (%)	55 ± 5	52 ± 7	50 ± 6	0.3	0.03	0.5
RV-EDV (ml/m ²)	105 ± 14	114 ± 26	119 ± 20	0.3	0.07	0.5
RV mass (g/m ²)	A0 ± 2	30 ± 7	33 ± 6	< 0.001	< 0.000	0.5
D _{proximal} (mm)	23 ± 3	18 ± 5	22 ± 2	< 0.001	0.4	0.002
D _{distal} (mm)	23 ± 2	18 ± 4	23 ± 3	< 0.001	0.4	< 0.001
D _{mid} (mm)	23 ± 1	19 ± 6	25 ± 5	< 0.001	0.02	0.005
Pulm _{dis} (cm)	1.7 ± 0.5	0.02 ± 0.09	1.8 ± 0.5	< 0.001	0.7	< 0.001
QF-PA (ml/heart beat)	75 ± 15	80 ± 9	76 ± 11	0.9	0.9	0.8
WSR of aorta wall (sec ⁻¹)	16 ± 3	39 ± 22	8 ± 9	< 0.001	0.3	< 0.001
WSR of anterior wall (sec ⁻¹)	16 ± 4	38 ± 16	33 ± 19	0.001	0.009	0.6
WSR of lateral wall (sec ⁻¹)	15 ± 4	37 ± 21	16 ± 18	0.002	0.9	0.003
WSR of posterior wall (sec ⁻¹)	15 ± 3	34 ± 26	7 ± 5	0.004	0.3	< 0.001

RV: right ventricle, EF: ejection fraction, WSR: wall shear rate, QF = quantitative flow, D_{proximal}: pulmonary artery/conduit diameter at the pulmonary valve level, D_{distal}: pulmonary artery/conduit diameter just before the bifurcation, D_{mid}: pulmonary artery/conduit diameter at mid distance between D_{proximal} and D_{distal}, and QF-PA: quantitative flow of pulmonary artery. Pulm_{dis}= Pulmonary artery/conduit distension.

There was no difference between pulmonary Vmax measured by 4D flow and echocardiographic measurement (2.6 ± 0.6 m/sec vs. 2.5 ± 0.5 m/sec, respectively p = 0.6 in the Contegra® group, and 3.3 ± 0.6 m/sec vs. 3.4 ± 0.3 m/sec, respectively p = 0.6 in the Melody® group). (Figure 3) No correlation between pulmonary Vmax and the time after Contegra® conduit implantation (R = 0.28, p = 0.4), or Melody® valve implantation (R = 0.13, p = 0.6) was observed. Pulmonary flow was laminar with no visible vortex, and without angle deviation of the pulmonary flow from the midline in all subjects in the control group (100%) and 13 patients (87%) in the Contegra® group. The 2 patients (13%) in the Contegra® group with an asymmetric conduit valve opening, and all the Melody® group patients (100%) had an eccentric flow towards the anterior wall with a deviation angle from the midline of 31 ± 10°. Vortices were seen in all patients with eccentric flow. (Figure 4, movie 1) Vortex size was positively correlated with pulmonary flow deviation angle (R = 0.97, p < 0.001) and with pulmonary Vmax (R = 0.54, p = 0.02).

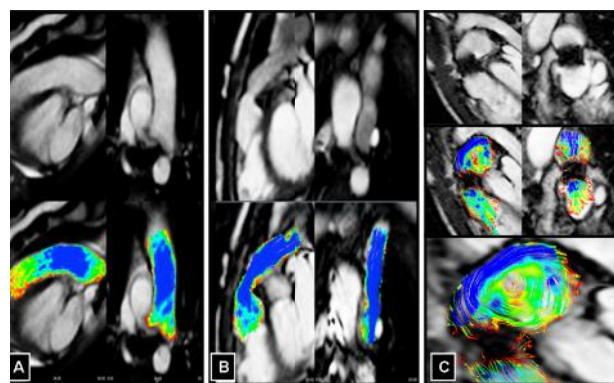


Figure 4 (A) Pulmonary artery in a normal subject; upper left (sagittal view), and upper right (coronal view). (B) Contegra® conduit; upper left (sagittal view), upper right (coronal view). Lower rows show traces of color-coded streamlines demonstrating laminar flow, no visible vortex, and no deviation of the flow from the mid line. (C) Melody® valve, upper left (sagittal view), upper right (coronal view). Middle rows show traces of colour-coded streamlines demonstrating eccentric flow, pulmonary flow is deviated from the midline, and vortex is seen. The lower rows are magnification of the vortex in a phase with the maximal vortex diameter.

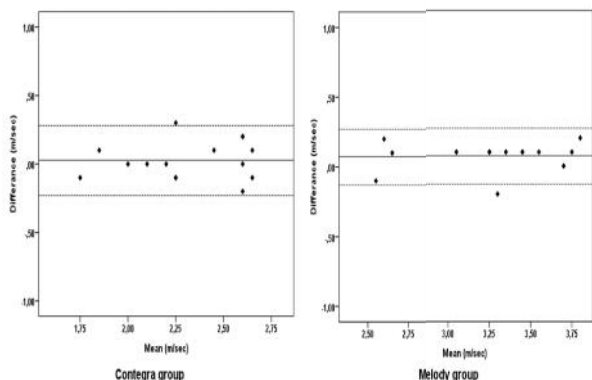


Figure 3 Bland Altman plot that show comparison maximum pulmonary flow velocity measured by 4D flow and echocardiographic measurements in Contegra and in Melody groups.

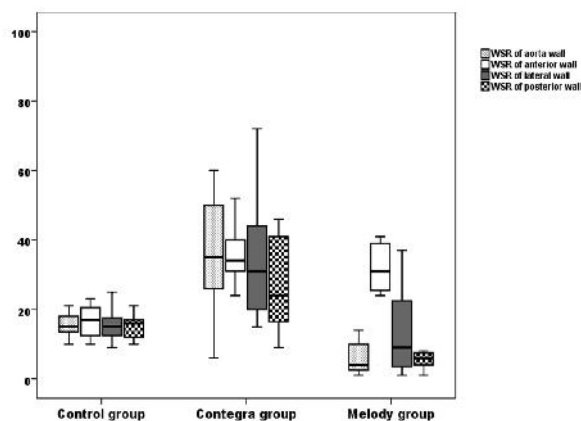


Figure 5 Box plot shows the wall shear rate (WSRs) in the three groups.

DISCUSSION

Here we show that pulmonary flow patterns differ significantly between patients with a surgical and percutaneously implanted bovine jugular venous valve in the RVOT. We found that all patients in Melody® group showed an eccentric pulmonary flow with vortex formation and a significant asymmetric elevated WSR at focal regions of the conduit. In contrast, those in Contegra® group and with symmetrical opening of the conduit valve showed a laminar pulmonary flow with no visible vortex and symmetric (although elevated) WSR values. Vortex formation leads to generation of dynamic actions on the surrounding structures and energy loss in forward flow. A vortex may thus be considered as an obstacle that partially obstructs the free flowing of the fluid inside a vessel. In the absence of any vortex formation, pressure would change as dictated by the Bernoulli balance. However, development of a vortex provokes an additional pressure drop (or energy loss) due to the transformation of energy into vortex inertia.²⁰ These abnormal hemodynamics due to the vortex formation distal to the percutaneous implanted valve might be related to lower RV systolic function in the patients who underwent Melody® implantation. The asymmetric elevated WSR values were related to the pulmonary flow jet direction (the direction of the jet matched the regions with elevated WSR values). The eccentric flow could lead to changes in endothelial function, a predisposing factor for vascular remodeling and great vessel dilatation.²¹⁻²³ Although still controversial, changes in WSR values have been suggested to play a role in the development and growth of aneurysms.²⁴ Previous studies reported that an asymmetric elevated WSR may be regarded as a trigger for aneurysmal formation in the ascending aorta of patients with a bicuspid aorta valve exhibiting eccentric aorta flow.^{25,26} Francois *et al*,²⁷ confirmed the presence of vortices in the dilated segments of the pulmonary artery in surgical corrected TOF patients.

Elevated but symmetrical WSR values in the Contegra® group are probably caused by the smaller lumen size and impaired distension of the venous conduit. Guber *et al*²⁸ suggested that the foreign body reaction (excessive intimal peel formation, severe perigraft scarring reaction, fibrointimal proliferation) on the outside layer of the Contegra® conduit could lead to an increase in stiffness of the Contegra® conduit and therefore, impaired elasticity of the conduit.

The hypertrophied RV in both patients groups, as compared to the controls, is probably caused by the underlying disease and past pressure overload but probably also due to higher resistance to outflow; in the Contegra® group due to relatively narrow unelastic conduits, and in the Melody® group due to unfavorable flow patterns with vortex formation distal from the Melody® valve.

It is worth mentioning that, in this study, the maximum flow velocities across the pulmonary valve determined by 4D flow were comparable to those determined by echocardiography. An important pitfall of standard 2D phase contrast magnetic resonance flow mapping is underestimation of the maximum flow velocity.²⁹ More studies may help to validate this concept especially within the context of stenotic valves.

Similar to previous publications,^{27;30;31} normal healthy volunteers in this study exhibited a laminar pulmonary flow pattern with no visible vortex. Our findings contradict with findings of Bachler *et al*, who demonstrated two counter-rotating vortices in the pulmonary flow of healthy volunteers.³² However, a difference in vortex definition might explain this contradiction. Bachler *et al* defined the vortex as a rotation or swirling motion in the flow field, while in our study and in other studies,^{27;30;31} a vortex was defined as a regional circular flow pattern deviating by more than 90° from the physiological flow direction along the vessel lumen.

Study Limitations

The relatively small number of patients in the cohort limits this study. Larger patient cohorts and more long term studies will be essential to learn more about the pathophysiological changes. A further difficulty of the 4D flow sequence is the long overall scan times of about 20 minutes. However, future improvement in scanning techniques will lead to a reduction in scanning time and hopefully the widespread use of 4D flow may help to unravel the complex flow patterns after surgery for congenital heart disease.

CONCLUSION

Pulmonary flow patterns differ significantly between patients with a surgical and percutaneously implanted bovine jugular venous valve in the RVOT. Unfavorable pulmonary flow patterns with vortex formation distal from the Melody® valve lead to abnormal hemodynamics that may influence RV function and might be a predisposing factor for a pulmonary aneurysm formation. Longer follow up studies are required to determine the implications of such knowledge for prognosis and therapy.

Reference

1. Chaturvedi RR, Redington AN: Pulmonary regurgitation in congenital heart disease. *Heart* 2007; 93:880-889.
2. Snellen HA, Hartman H, Buis-Liem TN, Kole EH, Rohmer J: Pulmonic stenosis. *Circulation* 1968; 38:93-101.
3. Haddad F, Doyle R, Murphy DJ, Hunt SA: Right ventricular function in cardiovascular disease, part II: pathophysiology, clinical importance, and management of right ventricular failure. *Circulation* 2008; 117:1717-1731.
4. Coats L, Khambadkone S, Derrick G, Sridharan S, Schievano S, Mist B, Jones R, Deanfield JE, Pellerin D, Bonhoeffer P, Taylor AM: Physiological and clinical consequences of relief of right ventricular outflow tract obstruction late after repair of congenital heart defects. *Circulation* 2006; 113:2037-2044.
5. Bonhoeffer P, Boudjemline Y, Qureshi SA, Le BJ, Iserin L, Acar P, Merckx J, Kachaner J, Sidi D: Percutaneous insertion of the pulmonary valve. *J Am Coll Cardiol* 2002; 39:1664-1669.
6. Khambadkone S, Coats L, Taylor A, Boudjemline Y, Derrick G, Tsang V, Cooper J, Muthurangu V, Hegde SR, Razavi RS, Pellerin D, Deanfield J, Bonhoeffer P:

- Percutaneous pulmonary valve implantation in humans: results in 59 consecutive patients. *Circulation* 2005; 112:1189-1197.
7. Lurz P, Coats L, Khambadkone S, Nordmeyer J, Boudjemline Y, Schievano S, Muthurangu V, Lee TY, Parenzan G, Derrick G, Cullen S, Walker F, Tsang V, Deanfield J, Taylor AM, Bonhoeffer P: Percutaneous pulmonary valve implantation: impact of evolving technology and learning curve on clinical outcome. *Circulation* 2008; 117:1964-1972.
 8. Romeih S, Kroft LJ, Bokenkamp R, Schaliij MJ, Grotenhuis H, Hazekamp MG, Groenink M, de RA, Blom NA: Delayed improvement of right ventricular diastolic function and regression of right ventricular mass after percutaneous pulmonary valve implantation in patients with congenital heart disease. *Am Heart J* 2009; 158:40-46.
 9. Frydrychowicz A, Berger A, Russe MF, Stalder AF, Harloff A, Dittrich S, Hennig J, Langer M, Markl M: Time-resolved magnetic resonance angiography and flow-sensitive 4-dimensional magnetic resonance imaging at 3 Tesla for blood flow and wall shear stress analysis. *J Thorac Cardiovasc Surg* 2008; 136:400-407.
 10. Markl M, Kilner PJ, Ebbers T: Comprehensive 4D velocity mapping of the heart and great vessels by cardiovascular magnetic resonance. *J Cardiovasc Magn Reson* 2011; 13:7.
 11. Markl M, Chan FP, Alley MT, Wedding KL, Draney MT, Elkins CJ, Parker DW, Wicker R, Taylor CA, Herfkens RJ, Pelc NJ: Time-resolved three-dimensional phase-contrast MRI. *J Magn Reson Imaging* 2003; 17:499-506.
 12. Karau KL, Krenz GS, Dawson CA: Branching exponent heterogeneity and wall shear stress distribution in vascular trees. *Am J Physiol Heart Circ Physiol* 2001; 280:H1256-H1263.
 13. Reneman RS, Arts T, Hoeks AP: Wall shear stress--an important determinant of endothelial cell function and structure--in the arterial system in vivo. Discrepancies with theory. *J Vasc Res* 2006; 43:251-269.
 14. Lorenz CH, Walker ES, Morgan VL, Klein SS, Graham TP, Jr.: Normal human right and left ventricular mass, systolic function, and gender differences by cine magnetic resonance imaging. *J Cardiovasc Magn Reson* 1999; 1:7-21.
 15. Hudsmith LE, Petersen SE, Francis JM, Robson MD, Neubauer S: Normal human left and right ventricular and left atrial dimensions using steady state free precession magnetic resonance imaging. *J Cardiovasc Magn Reson* 2005; 7:775-782.
 16. Buonocore MH: Visualizing blood flow patterns using streamlines, arrows, and particle paths. *Magn Reson Med* 1998; 40:210-226.
 17. Bogren HG, Buonocore MH: Helical-shaped streamlines do not represent helical flow. *Radiology* 2010; 257:895-896.
 18. van der Hulst AE, Westenberg JJ, Kroft LJ, Bax JJ, Blom NA, de RA, Roest AA: Tetralogy of fallot: 3D velocity-encoded MR imaging for evaluation of right ventricular valve flow and diastolic function in patients after correction. *Radiology* 2010; 256:724-734.
 19. Stalder AF, Russe MF, Frydrychowicz A, Bock J, Hennig J, Markl M: Quantitative 2D and 3D phase contrast MRI: optimized analysis of blood flow and vessel wall parameters. *Magn Reson Med* 2008; 60:1218-1231.
 20. Arash Kheradvar, Gianni Pedrizzetti: *Vortex Dynamics; Vortex Formation in the Cardiovascular System*. Springer, 2012, pp 17-45.
 21. Frydrychowicz A, Arnold R, Hirtler D, Schlensak C, Stalder AF, Hennig J, Langer M, Markl M: Multidirectional flow analysis by cardiovascular magnetic resonance in aneurysm development following repair of aortic coarctation. *J Cardiovasc Magn Reson* 2008; 10:30.
 22. Biegling ET, Frydrychowicz A, Landgraf BR, Johnson KM, Wieben O, Francois CJ: In vivo 3-dimensional Magnetic Resonance Wall Shear Stress Estimation in Ascending Aortic Dilatation. *J Magn Reson Imaging* 2011; 33:589-597.
 23. Markl M, Draney MT, Hope MD, Levin JM, Chan FP, Alley MT, Pelc NJ, Herfkens RJ: Time-resolved 3-dimensional velocity mapping in the thoracic aorta: visualization of 3-directional blood flow patterns in healthy volunteers and patients. *J Comput Assist Tomogr* 2004; 28:459-468.
 24. Meng H, Wang Z, Hoi Y, Gao L, Metaxa E, Swartz DD, Kolega J: Complex hemodynamics at the apex of an arterial bifurcation induces vascular remodeling resembling cerebral aneurysm initiation. *Stroke* 2007; 38:1924-1931.
 25. Barker AJ, Markl M, Burk J, Lorenz R, Bock J, Bauer S, Schulz-Menger J, von Knobelsdorff-Brenkenhoff F: Bicuspid aortic valve is associated with altered wall shear stress in the ascending aorta. *Circ Cardiovasc Imaging* 2012; 5:457-466.
 26. Barker AJ, Lanning C, Shandas R: Quantification of hemodynamic wall shear stress in patients with bicuspid aortic valve using phase-contrast MRI. *Ann Biomed Eng* 2010; 38:788-800.
 27. Francois CJ, Srinivasan S, Schiebler ML, Reeder SB, Niespodzany E, Landgraf BR, Wieben O, Frydrychowicz A: 4D cardiovascular magnetic resonance velocity mapping of alterations of right heart flow patterns and main pulmonary artery hemodynamics in tetralogy of Fallot. *J Cardiovasc Magn Reson* 2012;14:16.
 28. Gober V, Berdat P, Pavlovic M, Pfammatter JP, Carrel TP: Adverse mid-term outcome following RVOT reconstruction using the Contegra valved bovine jugular vein. *Ann Thorac Surg* 2005;79:625-631.
 29. Lotz J, Meier C, Leppert A, Galanski M: Cardiovascular flow measurement with phase-contrast MR imaging: basic facts and implementation. *Radiographics* 2002; 22:651-671.
 30. Geiger J, Markl M, Jung B, Grohmann J, Stiller B, Langer M, Arnold R: 4D-MR flow analysis in patients after repair for tetralogy of Fallot. *Eur Radiol* 2011; 21:1651-1657.

31. Reiter G, Reiter U, Kovacs G, Kainz B, Schmidt K, Maier R, Olschewski H, Rienmueller R: Magnetic resonance-derived 3-dimensional blood flow patterns in the main pulmonary artery as a marker of pulmonary hypertension and a measure of elevated mean pulmonary arterial pressure. *Circ Cardiovasc Imaging* 2008; 1:23-30.
32. Bachler P, Pinochet N, Sotelo J, Crelier G, Irrarrazaval P, Tejos C, Uribe S: Assessment of normal flow patterns in the pulmonary circulation by using 4D magnetic resonance velocity mapping. *Magn Reson Imaging* 2013; 31:178-188.

How to cite this article:

Soha Romeih *et al.* 2015, Nonuniformly Distributed Flow Patterns After Melody® Implantation: Implications for Focal Elevated pulmonary Wall Shear Rates and Right Ventricular Function. *Int J Recent Sci Res* Vol. 6, Issue, 10, pp. 6774-6780.

*International Journal of Recent Scientific
Research*

ISSN 0976-3031



9

770576

303009